Morphology and Crystal Structure of Solution-Grown Single Crystals of Poly[(*R*)-3-hydroxyvalerate]

Tadahisa Iwata* and Yoshiharu Doi

Polymer Chemistry Laboratory, RIKEN Institute, Hirosawa, Wako-shi, Saitama 351-0198, Japan

Received February 1, 2000; Revised Manuscript Received May 16, 2000

ABSTRACT: Solution-grown lamellar single crystals of bacterial poly[(*R*)-3-hydroxyvalerate] (P([*R*]-3HV)) have been prepared in a mixture of chloroform and methanol. P([*R*]-3HV) crystals were square-shaped and gave well-resolved electron diffraction diagrams from which the reciprocal lattice parameters $a^* = 1.052\ \mathrm{nm}^{-1}$, $b^* = 0.990\ \mathrm{nm}^{-1}$, and $\gamma^* = 90°$ could be determined. Systematic absences were confirmed at every odd reflection along the orthogonal axes a^* and b^* by a series of tilted electron diffraction diagrams. Thus, the electron diffraction pattern is consistent with a p_{2gg} symmetry. The diffraction analysis combined with X-ray and electron diffraction diagrams indicated that P([*R*]-3HV) crystallized in the $P2_12_12_1$ orthorhombic space group which had the lattice parameters of $a = 0.950$ nm, $b = 1.010$ nm, and c(fiber axis) $= 0.556$ nm with the 2-fold screw symmetry along the molecular axis. The growth planes of P([*R*]-3HV) single crystals are {110}, and the average direction of chain folding determined by polyethylene decoration is parallel to these growth planes. In some cases, the lamellar crystals showed spiral growths originating from screw dislocations with both left-handed and right-handed forms. Lateral force mode image of atomic force microscopy showed the "cross-sector" morphology which was due to differences in the chain-folding direction.

Introduction

Poly([*R*]-3-hydroxybutyrate) (P([*R*]-3HB)) is a biodegradable thermoplastic synthesized by various microorganisms.[1−3] It is well-known that P([*R*]-3HB) has a perfectly isotactic structure with only the *R* configuration.[4−6] The molecular and crystal structure of P([*R*]-3HB) has been determined by X-ray fiber diagrams and by energy calculation of the molecular chains, and it was revealed that two antiparallel chains in the left-handed helix conformation are packed in an orthorhombic unit cell with space group $P2_12_12_1$.[7,8] Besides that, the lamellar structure of solution-grown single crystals of P([*R*]-3HB) has also been extensively studied by using transmission electron microscopy and atomic force microscopy.[9−15]

However, despite showing the same biodegradable thermoplastic properties as P([*R*]-3HB),[16] the crystal and lamellar structure of poly([*R*]-3-hydroxyvalerate) (P([*R*]-3HV)) has not been investigated in detail. The crystal and molecular structure of the chemosynthesized racemic poly([*R*,*S*]-3-hydroxyvalerate) (P([*R*,*S*]-3HV)) was first studied by X-ray diffraction.[17] P([*R*,*S*]-3HV) crystallized into an orthorhombic form with the following unit cell parameters: $a = 0.932$ nm, $b = 1.002$ nm, and c(fiber axis) $= 0.556$ nm and the space group was $P2_12_12_1$. The unit cell contains two antiparallel chains in the 2/1 helix conformation. On the other hand, the elucidation of the crystal structure of naturally occurring P([*R*]-3HV) polymer was initially attempted by using the heteropolymer which is composed mainly of 3HV but contained a significant amount (approximately 20%) of 3HB. Based on the *d*-spacing of X-ray reflections, the unit cell parameters were found to be $a = 0.952$ nm, $b = 1.008$ nm, and c(fiber axis) $= 0.556$ nm.[18] Recently, pure P([*R*]-3HV) homopolymer production has been achieved by using several bacteria such as *Rhodococcus* sp.[19] and *Chromobacterium violaceum*.[20] Nevertheless, the complete analysis of pure P([*R*]-3HV) crystal structure has not been carried out.

Single crystals of bacterial and synthetic poly(3-hydroxyvalerate) (P(3HV)) were first prepared from boiling methanol by slow cooling of the solution by Marchessault et al.[18,21] They reported that the observed unit cell parameters were identical to those derived from X-ray fiber diffraction, and the morphology of synthetic P(3HV) single crystals had lower perfection than those from bacterial samples. More recently, the lamellar morphology of solution-grown single crystals, which have spiral terraces due to screw dislocations of either handedness, has been studied in order to understand the relationship between main-chain chirality and lamellar morphology.[22]

In this paper, we have attempted to obtain more insight into the crystal structure and the lamellar structure of solution-grown single crystals of P([*R*]-3HV) homopolymer by means of X-ray diffraction, transmission electron microscopy, and atomic force and lateral force microscopy.

Experimental Section

P(3HV) Samples. The bacterial poly([*R*]-3-hydroxyvalerate) (P([*R*]-3HV)) sample used in this study was isolated by Fukui et al. from a recombinant *Ralstonia eutropha* harboring the PHA-biosynthesis genes of *Aeromonas caviae*.[23] The weight-average molecular weight (M_w) and polydispersity (DPI) of this P([*R*]-3HV) sample was 1 760 000 and 2.8, respectively. For single-crystal preparation, the P([*R*]-3HV) sample was subjected to 1 N aqueous KOH alkaline hydrolysis with 18-crown-6 ether, according to a method reported previously.[24] To this end, 50 mg of P([*R*]-3HV) was dissolved in 8 mL of chloroform. After adding 2 mL of 1 N aqueous KOH and 40 mg of 18-crown-6 ether to the P([*R*]-3HV) solution, the mixture was stirred at 35 °C. The organic layer was then pipetted into a sample vessel and dried over anhydrous magnesium sulfate. After filtering, the organic layer was precipitated into methanol.

* To whom all correspondence should be addressed: Tel +81-48-467-9586; Fax +81-48-462-4667.

10.1021/ma000186m CCC: $19.00
Published on Web 07/08/2000

X-ray Analysis. The above-mentioned P([*R*]-3HV) was also used for the X-ray diffraction experiments. P([*R*]-3HV) films prepared by the slow evaporation of a solution in chloroform were oriented by stretching 800−1000% of their initial length by loosely hung weights in a silicone oil bath at 96 °C. To improve its crystallinity, the oriented P([*R*]-3HV) film was further annealed with weak tension at 90 °C for 24 h in an autoclave. X-ray fiber diagrams of P([*R*]-3HV) were recorded in a flat-plate camera on Fuji New RX films, using Ni-filtered Cu Kα radiation with a Rigaku D-9C type X-ray generator operated at 40 kV and 35 mA. The X-ray patterns were calibrated with CaF_2 powder.

Preparation of Single Crystals. The single crystals were grown in a mixture of chloroform and methanol. P([*R*]-3HV) (M_w = 260 000 and DPI = 1.6), which was prepared by alkaline hydrolysis with 18-crown-6 ether, was dissolved in chloroform at room temperature. To this solution was added warm methanol at 60 °C. The mixture was then quickly brought to 80 °C and maintained for 10 min, after which the temperature was slowly lowered to 60 °C. After 1 h at this temperature, the temperature was further lowered to 50 °C and maintained for 90 min, after which the heating element of the oil bath was turned off and the oil bath was allowed to cool slowly. The crystals were collected and washed by successive centrifugations first in mixture having the same solvent−precipitant ratio as in the mother liquor and then in ethanol.

Transmission Electron Microscopy. Drops of crystals suspension were deposited on carbon-coated grids, allowed to dry, and then shadowed with a Pt−Pd alloy. For electron diffraction purposes, the dried crystals were used directly without further treatments. The decoration of single crystals with polyethylene was performed by evaporating polyethylene on the crystals under vacuum according to the method described by Wittmann and Lotz[25] and then shadowed with a Pt−Pd alloy. These grids were observed with a JEM-2000FX II electron microscope operated at an acceleration voltage of 200 and 120 kV for electron diffraction and for the imaging of shadowed crystals, respectively. Additional information was obtained by sequentially tilting the crystals around a^* and b^* axes and recording a series of tilted electron diffraction diagrams. Most diffraction diagrams were recorded under cryo conditions at liquid nitrogen temperature. Calibration of the patterns was done at room temperature, after depositing the crystals on gold-coated grids. Electron diffraction diagrams and images were recorded on Kodak SO-163 and 4489 films, respectively, developed for 4 min with a Kodak D19 developer (diluted in water 1/2, v/v).

Atomic Force and Lateral Force Microscopy. The thicknesses and surface morphology of single crystals were investigated by atomic force microscopy (AFM) and lateral force microscopy (LFM). The AFM and LFM images were performed with a Seiko SPI3700/SPA300 Instrument. Pyramid-like Si_3N_4 tips, mounted on 100 μm triangle cantilevers with spring constants of 0.09 N/m, were applied for the contact mode experiment of AFM. Simultaneous registration was performed in the contact mode for height and deflection images. Pyramid-like Si_3N_4 tips, mounted on 100 μm long rectangular cantilevers with spring constants of 0.09 N/m, were applied for LFM experiment. For both AFM and LFM experiments, drops of crystal suspension were allowed to dry on mica. All images were recorded at room temperature.

Results and Discussion

Crystal Structure of P([*R*]-3HV). The X-ray fiber diagrams of the oriented P([*R*]-3HV) films annealed in an autoclave at 90 °C are shown in Figure 1. When 800% drawing was applied for P([*R*]-3HV) film, an arc reflection on the meridian of X-ray fiber diagram was observed as shown in Figure 1A. The fiber repeat distance of 0.502 nm calculated from this arc reflection on the meridian was not consistent with the values obtained from other layer reflections, suggesting that

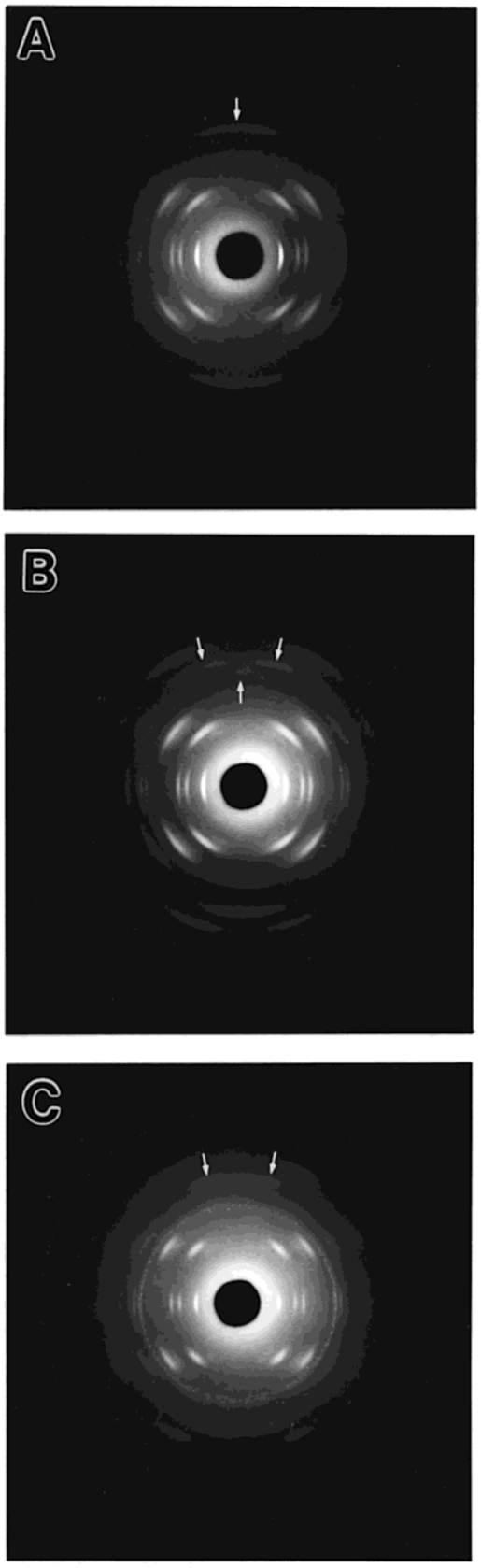

Figure 1. X-ray fiber diagrams of P([*R*]-3HV) annealed in an autoclave at 90 °C. The Debye−Scherrer ring of CaF_2 was used for calibration purposes: (A) 800% stretched film, arrow indicates the continuous diffuse scattering on the layer line; (B) tilted 800% stretched film, tilt angle is ca. 15°, arrows indicate discrete reflections on the layer line; and (C) 1000% stretched film, arrows indicate discrete reflections on the second layer line.

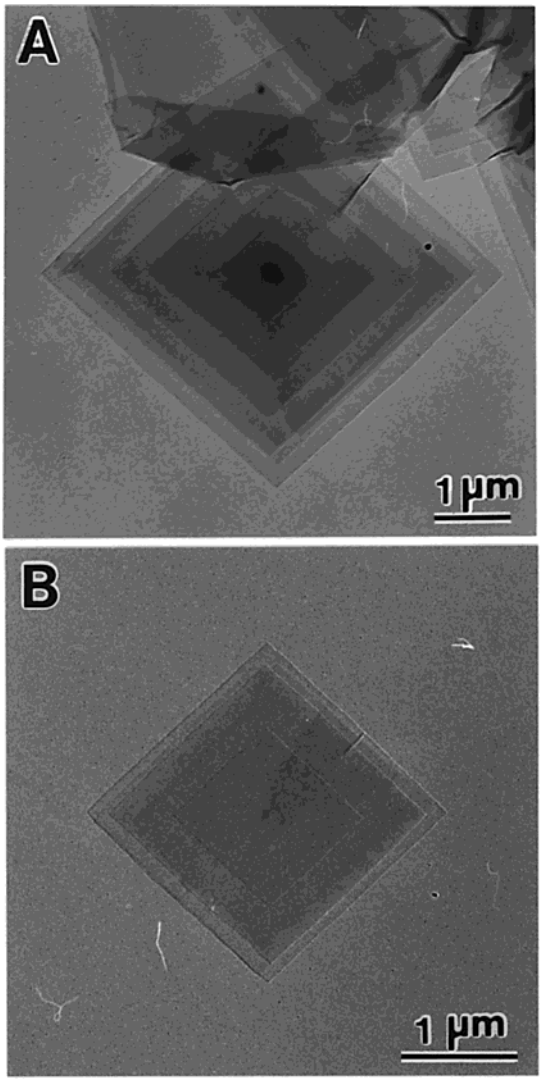

Figure 2. Electron micrographs after shadowing with Pt−Pd alloy of P([*R*]-3HV) single crystals grown in a mixture of chloroform and methanol: (A) 1/49: v/v and (B) 1/99: v/v.

this is not a real reflection on the meridian. When the film was slightly tilted against the X-ray beam, this meridian reflection on the second layer line was split into three reflections as shown in Figure 1B. The observed (002) reflection of the tilted fiber diagram indicates that the chain conformation of P([*R*]-3HV) is indeed a 2_1 helix. With further drawing up to 1000% of the initial length, the (002) reflection was not observed on the meridian of fiber diagram (Figure 1C), suggesting that 1000% drawing generates better orientation of P([*R*]-3HV) film. The fiber repeat distance was measured using all layer reflections of three pieces of X-ray fiber diagrams, and its average was 0.556 nm. This value is exactly the same as the fiber repeat distance of racemic P([*R,S*]-3HV) reported by Yokouchi et al.[17] and also P([*R*]-3HV) obtained from heteropolymer with approximately 20% β-hydroxybutyrate reported by Marchessault et al.[18]

Typical preparations of lamellar single crystals grown from a mixture of chloroform and methanol of 1/49 (v/v) or 1/99 (v/v) are shown in Figure 2. Both lamellar crystals occur as platelets of almost square shape with dimensions of around 2−4 μm. Large lamellar crystals from the solvent ratio of 1/49 (v/v) mainly contained many layers emanating from screw dislocations (Figure 2A), while smaller lamellar crystals obtained from solvent ratio 1/99 (v/v) shown in Figure 2B were observed as multilayer platelets without screw dislocation. The crystalline morphology of large lamellar crystals appeared to be less regular than in the case of small crystals. Small single crystals shown in Figure 2B gave well-resolved electron diffractograms compared to the larger lamellar crystals and were relatively stable under conditions of electron bombardment.

Each square-shaped single crystal yields a sharp electron diffraction pattern as shown in Figure 3. The diagram contains 48 independent reflections that are mirrored in the four quadrants defined along the two orthogonal reciprocal axes a^* and b^*. On the basis of the triple-exposure of the selected-area electron diffraction and the normal and selected-area images, it was confirmed that the lateral sides of crystals corresponded to the crystallographic {110} planes. All the equatorial reflections of the X-ray fiber diagram shown in Figure 1 are observed in electron diffraction pattern which confirms that the electron diffraction diagram is a projection along the *c*-axis: that is, the polymer chains align perpendicular to the lamellar base of the crystal. However, the X-ray pattern has a lower resolution than the electron diffraction pattern which displays diffraction spots down to 0.105 nm as opposed to only 0.320 nm for the X-ray pattern. Upon calibration of the electron diffraction pattern, the reciprocal lattice parameters were found to be $a^* = 1.052$ nm^{-1}, $b^* = 0.990$ nm^{-1}, and $\gamma^* = 90°$.

The two-dimensional space group of P([*R*]-3HV) was determined by base-plane electron diffractogram combined with the diagrams tilted around a^* and b^* axes. In the patterns shown in Figure 3, the forbidden spots 100, 300, 010, and 030 can be observed. However, in contrast to the electron diffraction, the presence of the forbidden diffraction spots could not be observed in X-ray fiber diagram. When the single crystal was tilted by 12° around b^*, the 010 and 030 spots disappeared completely as shown in Figure 3. Other experiments, giving similar results, were also achieved by tilting the crystals around a^* and observing the disappearance of 100 and 300. On the basis of the results of tilting trials, it is concluded that the two-dimensional space group symmetry is p_{2gg} which has systematic absences along a^* and b^* axes. Since the X-ray fiber pattern shows only even diffraction lines along the fiber axis and the electron diffraction pattern is consistent with p_{2gg} symmetry, it can be concluded that P([*R*]-3HV) crystals have the orthorhombic $P2_12_12_1$ space group.

In the diagram tilted by 40° shown in Figure 3, one sees a series of (2*k*1) spots 201, 211, and 221. The *d*-spacings of these reflections correspond to the values obtained from the X-ray fiber diagram, suggesting that P([*R*]-3HV) molecular chains align in single crystals with 2-fold screw symmetry along the molecular axis which has a fiber repeat distance of 0.556 nm. On the basis of all the reflection measurements of X-ray and electron diffraction patterns, it is concluded that P([*R*]-3HV) crystals have the orthorhombic form with the following unit cell parameters: $a = 0.950$ nm, $b = 1.010$ nm, and c(fiber axis) = 0.556 nm and the space group is $P2_12_12_1$. These values are in good agreement with those reported previously by Marchessault et al. for optically active P([*R*]-3HV) containing 20% 3HB units ($a = 0.952$ nm, $b = 1.008$ nm, and c(fiber axis) = 0.556 nm)[18] and for racemic P([*R,S*]-3HV) reported by Yok-

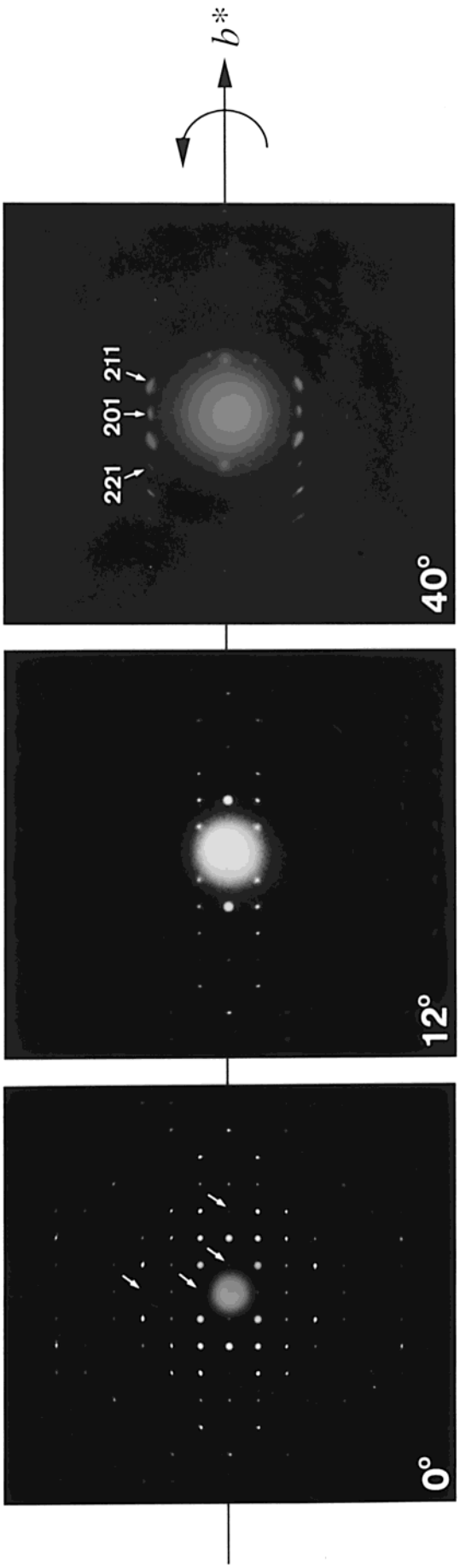

Figure 3. Typical electron diffraction pattern of base plane and electron diffraction diagrams obtained by tilting around b^* of a P([*R*]-3HV) single crystal as in Figure 2. The arrows indicate the forbidden spots along the a^* and b^* axes.

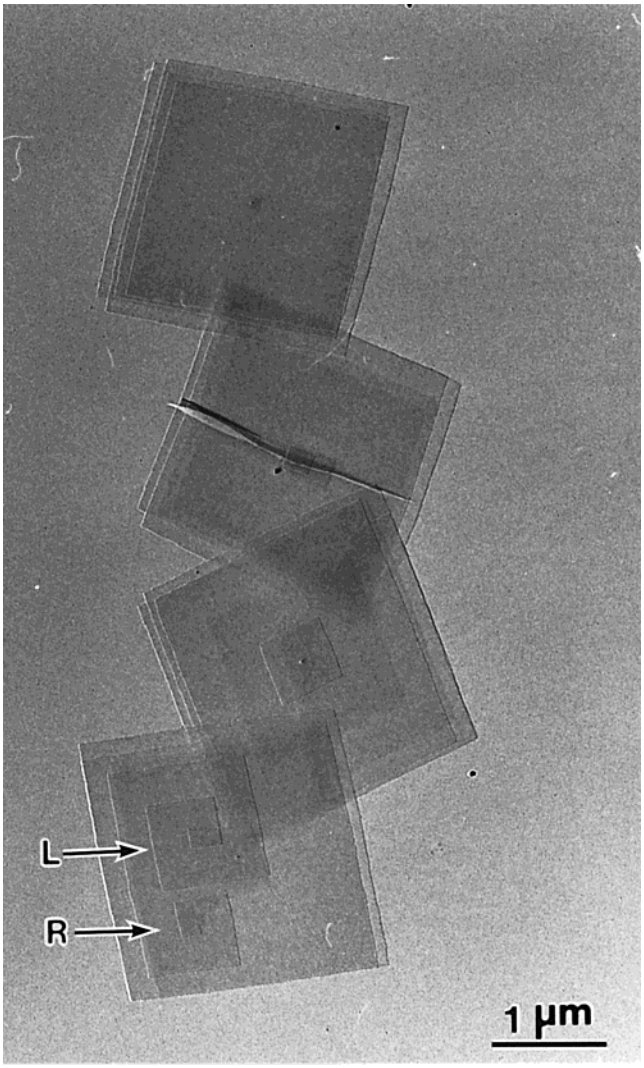

Figure 4. Lamellar morphology of P([*R*]-3HV) crystals in electron micrograph after shadowing with Pt−Pd alloy. Left-handed (L) and right-handed (R) screw dislocations could be observed in one lamellar crystal.

ouchi et al. (a = 0.932 nm, b = 1.002 nm, and c(fiber axis) = 0.556 nm).[17]

Surface Morphologies of Single Crystals. Figure 4 shows P([*R*]-3HV) single crystals with various surface morphologies. One morphology is shown as a multilamellar crystal while the other type of crystal shows spiral growth. In rare cases, one sees a pleat across the crystal as shown in Figure 4. Many lamellar crystals have one or two centrally located additional lamella on each side of the basal lamella. A small bump on the crystal surface can be observed in all of the crystals whose center is not complicated by spiral growth. This observation has been reported for single crystals of poly(3,3-bis(chloromethyl)oxacyclobutane) grown from dilute solution of xylene by Geil.[26] The author attributed this small bump to the primary nucleus of the crystal, which served as the nucleus for both the basal lamella and the additional lamellae.

Figure 5 shows AFM images of spiral grown crystals with right-handed or left-handed screw dislocations. Although the specimen was 100% isotactic with all of the asymmetric carbons in the *R* configuration, the P([*R*]-3HV) crystals had both the right-handed and left-handed screw dislocations in lamellar crystals. Furthermore, remarkably the screw dislocations of opposite

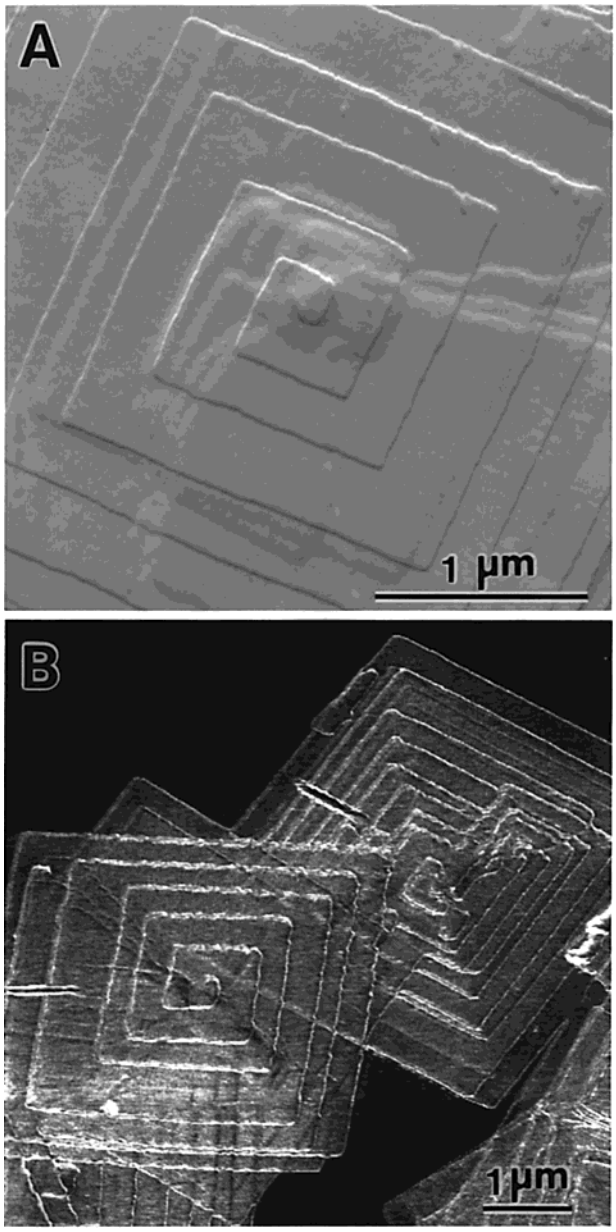

Figure 5. AFM images of P([*R*]-3HV) crystals with spiral terraces by screw dislocations of either handedness: (A) left-handed and (B) right-handed.

handedness occurred simultaneously in one lamellar crystal as shown in Figure 4. This incomprehensible phenomenon has not been reported before. However, recently we observed the same morphology in solution-grown single crystals of bacterial P([*R*]-3HB), which is a 100% isotactic biopolyester (unpublished data). The relationship between chirality and morphology has been extensively studied in banded spherulites. More recently, the relationship between main-chain chirality and the lamellar morphology of solution-grown single crystals has been investigated with (*R*)- and (*S*)-poly(epichlorohydrin), (*R*)- and (*S*)-poly(propylene oxide), and P([*R*]-3HV) by Saracovan et al.[22] They have concluded that the main-chain chirality may not contribute to establish the handedness of screw dislocation in lamellar crystals. Our results support their observation and indicate that the screw dislocations of opposite handedness can occur simultaneously even in one lamellar crystal.

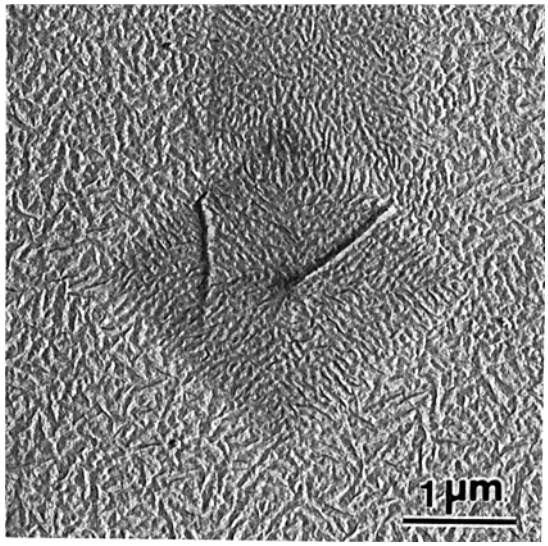

Figure 6. Typical electron micrograph of P([*R*]-3HV) single crystal decorated with polyethylene and shadowed with Pt−Pd alloy.

The energetically stable conformation of P([*R*]-3HB) single chain was first proposed as involving right-handed screw symmetry along the molecular axis by Okamura and Marchessault.[7] This conformation was reexamined by Cornibert and Marchessault,[27] and four energetically stable conformations (one was left-handed and three were right-handed) were obtained. Yokouchi et al. have independently found the six models, three left-handed helices and three right-handed helices, with plausible internal rotation angles.[8] Both groups finally determined that the crystal structure of P([*R*]-3HB) involved the left-handed molecular chain conformation. However, taking into consideration the result that there was a small difference in potential energy between the two helical forms, both right-handed and left-handed helical conformations could be possible energetically. The conformational analysis of P([*R*]-3HV) single chains has also been reported by Yokouchi et al.,[17] and it was revealed that four energetically stable conformations were found. These conformational variations of single chains might correspond to the handedness of screw dislocations in lamellar crystals grown from dilute solution under isothermal crystallization conditions.

Chain-Folding Structure. It is well-known that polyethylene[28−30] and polypropylene[31] have chain folding at lamellar surfaces, and also in the field of biodegradable aliphatic polyesters it is revealed that P([*R*]-3HB)[14,32] and poly(L-lactic acid)[33,34] crystallize with chain-folding structures. The measurement of lamellar thickness by atomic force microscopy and polyethylene decoration method are quite useful techniques for elucidating the chain-folding structure of lamellar single crystals and chain-folding direction on the crystal surface.

The lamellar thickness of P([*R*]-3HV) single crystals is about 5−6 nm as determined by AFM. Taking the fiber repeat distance of 0.556 nm and molecular weights into consideration, the chain foldings occur at the lamellar surfaces of P([*R*]-3HV) single crystals as it is with polyethylene[28,29] and P([*R*]-3HB)[14,32] single crystals. Figure 6 shows the P([*R*]-3HV) single crystals decorated with polyethylene and shadowed with Pt−Pd alloy. Slight orientation of the decorated crystals revealed the sectorization of the P([*R*]-3HV) single

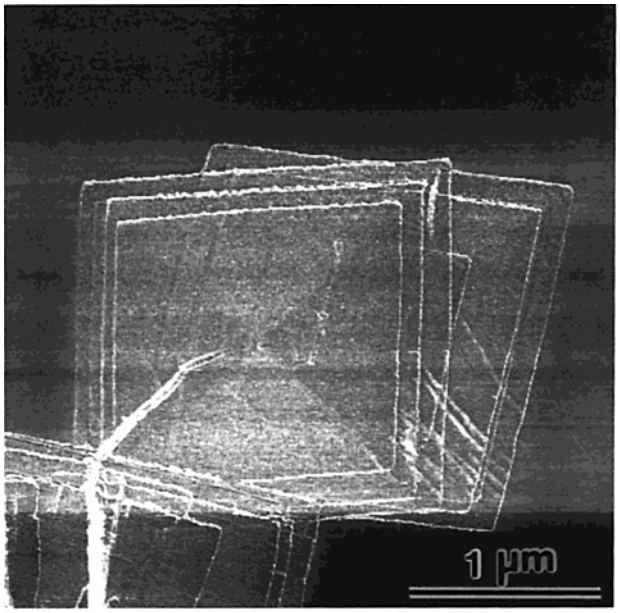

Figure 7. LFM image of P([*R*]-3HV) single crystals.

crystal into four quadrants. Polyethylene rod crystals are oriented perpendicular to the substrate {110} growth faces. This result indicates that the average direction of chain folding occurred along the {110} growth planes.

Figure 7 shows the LFM image with the sectorization of the P([*R*]-3HV) single crystal into four quadrants. This sectorization with a different contrast seems to correspond to a different value of lateral force and was the result of the scanning direction of the cantilever. When the scanning direction of the cantilever corresponded to the *a* or *b* axis of a single crystal, the sectorization could not be observed. However, when the scanning direction corresponded to the {110} growth planes, the sectorization into four quadrants could be observed as shown in Figure 7. Therefore, this sectorization is due to the folding direction of P([*R*]-3HV) chain boundaries. The LFM observation of polyethylene single crystals was reported by Kajiyama et al.,[35,36] and their observation for polyethylene single crystals was clearer than that of our P([*R*]-3HV) single crystals. This difference might be due to the difference in surface regularity between polyethylene and P([*R*]-3HV) single crystals. P([*R*]-3HV) contains the ethyl side groups with high mobility in the molecular main chain. Because of the free rotation of these side groups on the crystal surface, the surface regularity of P([*R*]-3HV) single crystals could be less than that of polyethylene crystals. The low regularity of P([*R*]-3HV) crystal surface is reflected by the low orientation of polyethylene crystals decorating the P([*R*]-3HV) single crystals as shown in Figure 6. Based on the TEM image shown in Figure 6 and the LFM image shown in Figure 7, the schematic display of chain-folding structure of P([*R*]-3HV) single crystals proposed in this study is presented in Figure 8.

Conclusion

The crystal structure of bacterial poly([*R*]-3-hydroxyvalerate) (P([*R*]-3HV)) has been determined by the analysis of X-ray fiber diagrams and electron diffraction patterns of a single-crystal specimen. The unit cell of P([*R*]-3HV) is orthorhombic with space group $P2_12_12_1$ and parameters $a = 0.950$ nm, $b = 1.010$ nm, and c(fiber axis) $= 0.556$ nm. Lamellar single crystals grown in a mixture of chloroform and methanol were square-shaped and thickened by a screw dislocation mechanism with both left-handed and right-handed forms. The growth planes of single crystals are {110}, and the average direction of chain folding is parallel to these growth planes as confirmed by the electron micrographs of single crystals decorated with polyethylene and lateral force microscopic observation. Lateral force microscopic image revealed cross-sector observation which was due to differences in chain-folding direction.

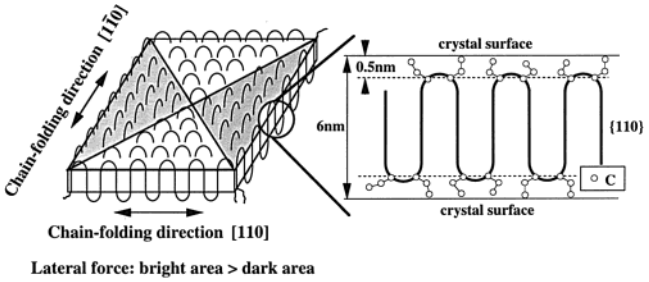

Figure 8. Schematic representation of P([*R*]-3HV) single crystals with chain folding along {110} growth planes proposed in this study.

Acknowledgment. The authors thank Dr. T. Fukui for providing the sample used in this study. We appreciate the assistance provided by Dr. K. Sudesh for the English correction of our manuscript. This work has been supported by a grant for Ecomolecular Science Research provided to RIKEN Institute by the Science and Technology Agency (STA) of Japan and in part by the Science Research Fund of Ministry of Education, Science and Culture of Japan (No. 11750784).

References and Notes

(1) Dawes, E. A.; Senior, P. J. *Adv. Microb. Physiol.* **1973**, *10*, 135.
(2) Anderson, A. J.; Dewes, E. A. *Microbiol. Rev.* **1990**, *54*, 450.
(3) Doi, Y. *Microbial Polyesters*; VCH Publishers: New York, 1990.
(4) Lemoignei, M. *Ann. Inst. Pasteur* **1925**, *39*, 144.
(5) Lemoignei, M. *Ann. Inst. Pasteur* **1927**, *41*, 148.
(6) Alper, R.; Lundgren, D. G.; Marchessault, R. H.; Côté, W. A. *Biopolymers* **1963**, *1*, 545.
(7) Okamura, K.; Marchessault, R. H. In *Conformation of Biopolymer*; Ramachandran, G. N., Ed.; Academic Press: London, 1967; Vol. 2, pp 709−720.
(8) Yokouchi, M.; Chatani, Y.; Tadokoro, H.; Teranishi, K.; Tani, H. *Polymer* **1973**, *14*, 267.
(9) Lundgren, D. G.; Alper, R.; Schnaitman, C.; Marchessault, R. H. *J. Bacteriol.* **1965**, *89*, 245.
(10) Marchessault, R. H.; Coulombe, S.; Morikawa, H.; Okamura, K.; Revol, J.-F. *Can. J. Chem.* **1981**, *59*, 38.
(11) Mitomo, H.; Barham, P. J.; Keller, A. *Polym. J.* **1987**, *19*, 1241.
(12) Seebach, D.; Bürger, H. M.; Müller, H. M.; Lengweiler, U. D.; Beck, A. K.; Sykes, K. E.; Barker, P. A.; Barham, P. J. *Helv. Chim. Acta* **1994**, *77*, 1099.
(13) Marchessault, R. H.; Bluhm, T. L.; Deslandes, Y.; Hamer, G. K.; Orts, W. J.; Sundararajan, P. R.; Taylor, M. G.; Bloembergen, S.; Holden, D. A. *Makromol. Chem., Macromol. Symp.* **1988**, *19*, 235.
(14) Birley, C.; Briddon, J.; Sykes, K. E.; Barker, P. A.; Organ, S. J.; Barham, P. J. *J. Mater. Sci.* **1995**, *30*, 633.
(15) Iwata, T.; Doi, Y.; Tanaka, T.; Akehata, T.; Shiromo, M.; Teramachi, S. *Macromolecules* **1997**, *30*, 5290.
(16) Nobes, G. A. R.; Marchessault, R. H.; Briese, B. H.; Jendrossek, D. *J. Environ. Polym. Degrad.* **1998**, *6*, 99.
(17) Yokouchi, M.; Chatani, Y.; Tadokoro, H.; Tani, H. *Polym. J.* **1974**, *6*, 248.

(18) Marchessault, R. H.; Morikawa, H.; Revol, J.-F.; Bluhm, T. L. *Macromolecules* **1984**, *17*, 1882.
(19) Haywood, G. W.; Anderson, A. J.; Williams, D. R.; Dawes, E. A. *Int. J. Biol. Macromol.* **1991**, *13*, 83.
(20) Steinbüchel, A.; Debzi, E.-M.; Marchessault, R. H.; Timm, A. *Appl. Microbiol. Biotechnol.* **1993**, *39*, 443.
(21) Marchessault, R. H.; Debzi, E. M.; Revol, J. F.; Steinbüchel, A. *Can. J. Microbiol.* **1995**, *41* (Suppl. 1), 297.
(22) Saracovan, I.; Cox, J. K.; Revol, J.-F.; Manley, R. St. J.; Brown, G. R. *Macromolecules* **1999**, *32*, 717.
(23) Fukui, T.; Kichise, T.; Yoshida, Y.; Doi, Y. *Biotechnol. Lett.* **1997**, *19*, 1093.
(24) Iwata, T.; Doi, Y.; Kasuya, K.; Inoue, Y. *Macrmolecules* **1997**, *30*, 833.
(25) Wittmann, J. C.; Lotz, B. *J. Polym. Sci., Polym. Phys. Ed.* **1985**, *23*, 205.
(26) Geil, P. H. *Polymer* **1963**, *4*, 404.
(27) Cornibert, J.; Marchessault, R. H. *J. Mol. Biol.* **1972**, *71*, 735.
(28) Reneker, D. H.; Geil, P. H. *J. Appl. Phys.* **1960**, *31*, 1916.
(29) Khoury, F.; Padden, F. J., Jr. *J. Polym. Sci.* **1960**, *47*, 455.
(30) Geil, P. H. *Polymer Single Crystals*; Interscience Publishers: New York, 1963.
(31) Sauer, J. A.; Morrow, D. R.; Richardson, G. C. *J. Appl. Phys.* **1965**, *36*, 3017.
(32) Iwata, T.; Doi, Y.; Kokubu, F.; Teramachi, S. *Macrmolecules* **1999**, *32*, 8325.
(33) Kalb, B.; Pennings, A. J. *Polymer* **1980**, *21*, 607.
(34) Iwata, T.; Doi, Y. *Macromolecules* **1998**, *31*, 2461.
(35) Kajiyama, T.; Ohki, I.; Takahara, A. *Macromolecules* **1995**, *28*, 4768.
(36) Kajiyama, T.; Fujii, T.; Takahara, A. *Polym. Prepr.* **1998**, *39*, 1179.

MA000186M